Margin-to-Failure Calculations for the TMI-2 Vessel[a]

By J. Rempe,[b] L. Stickler,[b] S. Chàvez,[b] G. Thinnes,[b] R. Witt,[c] and M. Corradini[c]

Abstract: *As part of the Three Mile Island Unit 2 (TMI-2) Vessel Investigation Project (VIP) sponsored by the Organization for Economic Cooperation and Development (OECD), margin-to-failure (MTF) calculations for mechanisms having the potential to threaten the integrity of the vessel lower head were performed to better understand events that occurred during the TMI-2 accident. Analyses considered four failure mechanisms: penetration tube rupture, penetration tube ejection, global vessel rupture, and localized vessel rupture. Calculational input was based on data from the TMI-2 VIP examinations of the vessel steel samples, penetration tube nozzles, and samples of the hard layer of debris found on the TMI-2 vessel lower head. Sensitivity studies were performed to investigate the uncertainties in key parameters for these analyses. Calculation results indicate that less margin existed for vessel failure mechanisms, rather than tube failure mechanisms, during the TMI-2 accident. In addition, calculations suggest that additional experimental data are needed to reduce uncertainties in models for predicting debris cooling and vessel failure.*

On March 28, 1979, the Three Mile Island Nuclear Station Unit 2 (TMI-2) pressurized-water reactor underwent a prolonged, small-break loss-of-coolant accident that severely damaged the reactor core. The postulated end-state conditions of the TMI-2 reactor vessel and core are shown in Fig. 1. As illustrated in this figure, at least 45% of the core melted. Video examinations after the accident indicate that approximately 19 000 kg of molten material relocated from the core region to the water-filled, lower head of the reactor vessel. Examinations indicate that relocated debris severely ablated several instrument tube penetrations inside the lower head, although instrument tubes appeared to be protected at the point where they were welded to the lower head. Instrument tubes outside the vessel and the vessel lower head, however, remained intact throughout the accident. Metallurgical examinations indicate that a localized region of the vessel, approximately 1 m by 0.8 m, reached temperatures between 1075 and 1100 °C during the accident; these examinations also indicate that vessel temperature away from the hot spot did not exceed 727 °C during the accident. However, these temperatures are well above the 538 °C maximum operating temperature limit considered in Case N-499 of the American Society of Mechanical Engineers (ASME) Boiler and Pressure Vessel Code.[1]

As part of the TMI-2 Vessel Investigation Project (VIP), margin-to-failure (MTF) analyses were performed to increase understanding of the events that occurred during the TMI-2 accident. Calculations were performed considering four vessel lower-head failure mechanisms: penetration tube rupture, penetration tube ejection, global vessel rupture, and localized vessel rupture. Although experimental data have validated many aspects of severe accident analyses models, no integral experimental data are available to validate entire models. Hence the data available from the TMI-2 VIP, previous TMI-2 research programs, and plant instrumentation provide a unique opportunity to assess uncertainties in severe accident analyses models.

This article summarizes models used in the MTF analysis effort. Significant results from these calculations are also presented. A more complete description of the analyses and results can be found in Ref. 2.

APPROACH

Figure 2 depicts the four failure mechanisms considered in these analyses. The tube rupture failure mechanism (part a of Fig. 2) may result from a combination of high pressure and elevated ex-vessel tube temperatures as the result of contact with debris that has traveled through the tube to ex-vessel locations. Failure of a penetration tube weld (part b of Fig. 2) could result from

[a]The U.S. Nuclear Regulatory Commission supported this work in conjunction with OECD, through DOE Contract DE-AC07-76IDO1570.

[b]Idaho National Engineering Laboratory, P.O. Box 1625, Idaho Falls, Idaho 83415-3840.

[c]University of Wisconsin, Madison, Department of Nuclear Engineering and Engineering Physics, 153 Engineering Research Building, 1500 Johnson Drive, Madison, Wisconsin 53706-1687.

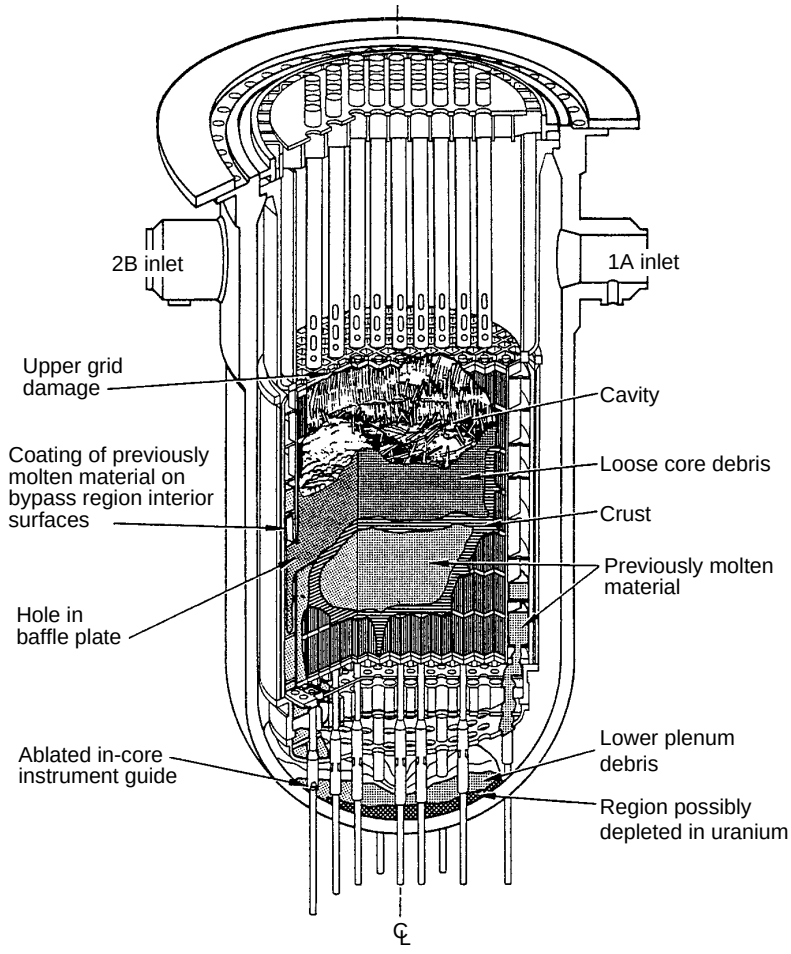

Fig. 1 Postulated TMI-2 end-state configuration.

debris melt attack and sustained heating from accumulated debris around the perimeter of a tube combined with reactor system pressure. Once the weld has failed, tube ejection is possible. Global vessel rupture (part c of Fig. 2) may be caused by elevated system pressure and/or the weight of debris on the lower head in conjunction with sustained heating from debris on the lower head. Localized vessel rupture (part d of Fig. 2) may be caused by thermal loads on the lower head as the result of nonuniform heat sources within the debris bed or a coherent jet of debris impinging directly onto the lower head in conjunction with mechanical loads caused by system pressure and debris weight.

As discussed previously, data from the TMI-2 VIP provide a unique opportunity to assess uncertainties in severe accident analysis tools. Little, if any, validation has been performed on methods used to predict melt–water interaction, molten pool behavior, cooling in debris that solidifies after relocation, and structural creep failure in a severe accident. Thus this calculational effort is useful not only because it provides insights into what failure mechanisms were plausible during the TMI-2 event and identifies the failure mode with the smallest margin during the TMI-2 event but also because it indicates areas where additional data are needed for severe accident modeling.

Calculations relied on VIP examination data from the TMI-2 instrument nozzles, the hard layer of debris found on the head (the “companion debris samples”), and the TMI-2 reactor vessel steel (the “vessel boat samples”). Metallurgical examination data were used to characterize peak vessel temperatures, the duration of

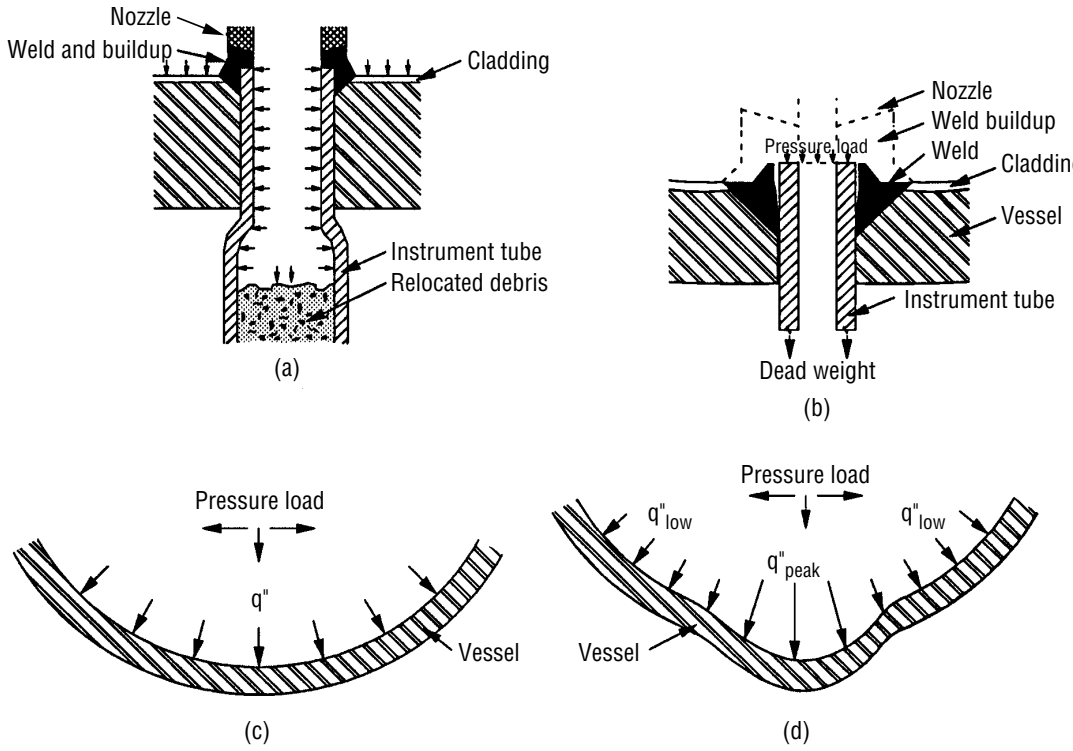

Fig. 2 Failure mechanisms considered in TMI-2 MTF analyses: (a) tube rupture, (b) weld failure–tube ejection, (c) global vessel failure, and (d) localized vessel failure.

peak temperatures, vessel cooling rates, and the end state of instrument nozzle weld material.[3,4] Data from examinations of companion debris samples were used to characterize such debris properties as decay heat and material composition.[5] Nozzle examination data were used to characterize the composition of melt attached to nozzles, elevations for nozzle ablation heights in the vessel, and melt penetration distances within nozzles.[6] Uncertainties for each data source are discussed in Ref. 2. Calculations included sensitivity studies to consider the range of input associated with uncertainties in data.

The potential for each failure mechanism to occur was evaluated on the basis of both ultimate strength and creep damage. Ultimate strength MTF was defined by

$$\text{MTF} = (1 - \text{effective stress/ultimate strength})\ 100\%$$

The TMI-2 Structural Mechanics Peer Review Group defined by consensus a separate stress-based MTF for creep failure.[7] The procedure includes converting multidimensional stress history to an effective stress (equivalent uniaxial stress) history and predicting time to failure for the converted stress and temperature histories using a time-damage model. When results from the initial scoping calculations suggested that a stress-based failure criterion may be too conservative for the prediction of failure, calculations were performed in which creep failure was defined as the point at which strain instability occurred (strain rate approaches infinity).[8]

The MTF calculations investigated an inconsistency between companion debris sample data, which suggest slow debris cooling, and vessel steel sample examination data, which imply relatively fast vessel cooling rates. When results primarily obtained from input based on companion debris sample data indicated that vessel failure would occur, irrespective of which failure criterion was selected, it was postulated that additional cooling (not currently modeled in severe accident analysis codes) occurred. A thermal analysis based on plant thermal hydraulic parameters measured or inferred from data measured during the accident [coolant temperature, reactor coolant system (RCS) pressure, cool-

ant flow rates entering and exiting the vessel, etc.] confirmed that more cooling than currently considered in severe accident analysis codes occurred during the period between debris relocation and vessel repressurization. Hence calculations were performed to quantify the magnitude of this cooling and possible debris configurations that could explain how this cooling could have occurred.

HIGHLIGHTS FROM MTF ANALYSIS RESULTS

Results from scoping calculations, which evaluate each of the failure mechanisms identified are reviewed in the following text. Results from thermal analyses, required as input for structural response calculations, are also discussed. Finally, results from calculations performed to assess sensitivity to debris cooling rates and different failure criteria are presented.

Melt Penetration–Ex-Vessel Tube Rupture

For ex-vessel tube rupture to occur, melt must travel through an ablated instrument tube to a distance that is below the vessel outer surface in part a of Fig. 2. Several models have been developed to predict the penetration distance of molten debris through vessel instrumentation nozzles. Although previous research was insufficient to select a model for predicting melt flow through light-water-reactor instrument tubes, melt penetration distances have been experimentally determined to be bounded by distances predicted by the bulk-freezing model and the conduction heat transfer model. The bulk-freezing model, first advanced by Ostensen and Jackson,[10,11] assumes that turbulent heat transfer governs melt solidification and penetration behavior. The conduction heat transfer model, first advanced by Epstein,[12,13] assumes that (as its name implies) conduction heat transfer governs melt solidification and penetration behavior.

Data from some TMI-2 instrument nozzles provide measurable distances for melt that traveled through in-vessel instrument structures during the TMI-2 accident. Longer nozzles containing melt with measurable penetration distances were used to select an appropriate model for estimating penetration distances; this model was then used to determine if melt could travel below the vessel lower head through shorter nozzles (see Fig. 3). Melt penetration distances predicted with a bulk-freezing model,[9] modified to consider heat loss from the melt to the tube and the coolant, were found to be consistent with distances measured in TMI-2 instrument nozzles. Distances predicted with a conduction model,[12,13] on the other hand, were found to be much longer (typically, several orders of magnitude longer) than melt penetration distances measured in TMI-2 instrument nozzles. Hence the modified bulk-freezing model was determined to be more appropriate for estimating the melt penetration distances observed in the TMI-2 nozzles.

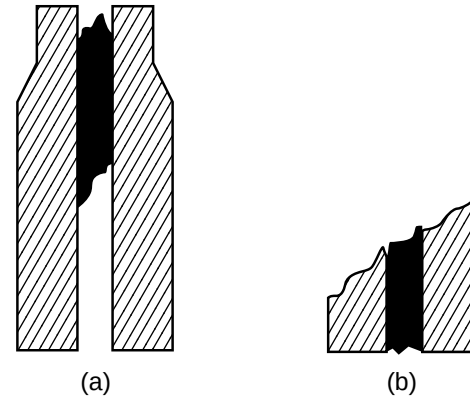

Fig. 3 Various configurations of melt observed in TMI-2 instrument nozzles: (a) nozzle stub containing melt with measurable penetration distance and (b) nozzle stub containing melt with unknown penetration distance.

Melt penetration distances predicted with the modified bulk-freezing model indicate that fuel containing molten debris would not travel through instrument tubes to locations below the lower head. Calculations bounded possible melt compositions, temperatures, and melt flow areas to maximize penetration distances. Furthermore, the nozzle stub height was assumed as 1.3 cm, which was the smallest ablated nozzle height observed in TMI-2 defueling efforts.[14] Although calculations indicate that it is possible for molten debris with highly metallic compositions to flow to ex-vessel tube locations, previous review of TMI-2 instrumentation data[15] suggests that metallic material quenched when it relocated to the lower head during the TMI-2 accident. Hence ex-vessel tube temperatures are not predicted to be higher than the RCS temperatures. Therefore ex-vessel tube rupture calculations were performed assuming that the tube temperatures were consistent with the vessel coolant temperatures.

A simple model comparing the pressure force on the tube and the tube's ultimate strength was used to evaluate ex-vessel tube rupture. As discussed previously, tube

temperatures for these analyses were assumed to equal the vessel coolant temperature. An upper bound on the coolant temperature was taken to be a representative saturation temperature (327 °C) corresponding to system pressures during the first 12 hours after the major relocation of fuel occurred; a lower-bound temperature was based on the minimum temperature (127 °C) measured in the cold legs during the transient. Although ultimate strength data for Inconel are limited,[9] data shown in Fig. 4 indicate that the ultimate strength for the TMI-2 Inconel instrument tubes is above 700 MPa for the temperatures of interest (127 to 327 °C). Because such temperatures were expected to result in very high MTFs, a conservatively high constant upper system pressure of 15 MPa was also applied in the tube rupture calculations. Thus calculations indicate that ultimate-strength MTF for tube temperatures of 127 and 327 °C are both above 95%. Times to creep rupture at these temperatures are estimated to be on the order of 10^{15} and 10^{29} hours. Hence ex-vessel tube rupture can effectively be eliminated as a potential failure mechanism for this accident.

Jet Impingement–Vessel Thermal Response

Calculations were performed to investigate melt relocation and the subsequent thermal loading to the vessel during the TMI-2 accident. Results from these calculations provide input to subsequent weld failure, global vessel failure, and localized failure analyses. Analytical models were applied to simulate the debris–vessel interaction to investigate the thermal response of the vessel during and after debris relocation. These models include phenomena such as breakup of melt relocating into and through the lower plenum water, growth of the debris pool and its associated top and bottom crusts, heat fluxes delivered to the vessel inner surface, and the resulting vessel temperature distribution. Because considerable uncertainty is associated with many input parameters for these models, studies were performed considering lower-bound, upper-bound, and best-estimate (or nominal) values for input parameters related to debris decay heat, debris relocation mass, and heat transfer from the debris and the vessel. Many of the input parameters for the thermal analysis were based on companion debris sample examination data (debris composition, decay heat levels, and "slow cooling" evidence).[5] Results from the thermal analyses were compared with results from vessel steel sample examinations (peak hot spot and global vessel temperatures, duration of peak hot spot temperatures, and cooling rate of vessel in the hot spot location).[4]

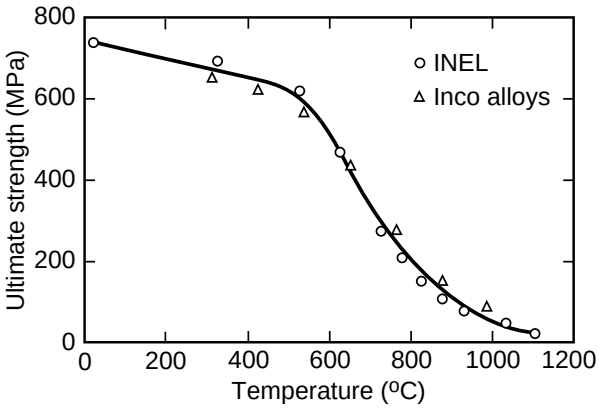

Fig. 4 Inconel-600 ultimate strength as a function of temperature.

The potential for melt to disperse and quench as it passes through the flow distributor plate and into the water-filled lower plenum was analyzed with the TEXAS fuel–coolant interaction (FCI) model.[16] TEXAS predicts the behavior of molten fuel interacting with water during the mixing and propagation phases of a molten FCI. As with many phenomena considered in severe accident analysis codes, considerable uncertainty may exist in TEXAS results because of limited data for validating FCI codes; however, various TEXAS sensitivity studies were used to address the impact of code modeling uncertainties. Sensitivity studies were also used to assess the impact of input data uncertainties. Posttest examination data and plant instrumentation data indicate that the major relocation of melt occurred within a 2-minute time period during the accident (224 to 226 minutes after reactor scram). Calculations considered total mass flow rates ranging from 300 to 1000 kg/s to address uncertainties in mass flow rates, although the duration of the jet pour was reduced to keep the total mass that relocated constant. Because melt may have drained from more than one of the holes in the elliptical flow distributor plate, analyses considered one and three jet cases. For all the cases, the system pressure was 10 MPa, which was the reactor vessel pressure during the time period when most debris relocation is postulated to have occurred. Jets were assumed to pour through coolant at saturated and subcooled conditions (the amount of subcooling was bounded by the temperatures measured in the RCS cold leg). The temperature of the melt at injection was assumed as 2630 °C, the liquidus temperature for the

composition of the melt identified in the companion sample examinations.[5]

Simulation results from the TEXAS fuel–coolant interaction model indicate that insignificant amounts of melt dispersal or "breakup" occur as melt relocates to the lower head. Maximum breakup was obtained for cases in which three jets were assumed to be present; however, even in these cases, less than 1% of the relocating material is estimated to break away from the jet and quench. When the breakup was predicted to be insignificant, the analyses of fuel relocation continued under the assumption that molten debris reached the lower plenum in a substantially liquid state, ultimately impinging on the vessel. Because vessel thermal response calculations indicate that the molten material that relocated to form the "hard layer" could, by itself, impose a thermal load resulting in temperatures that exceeded peak values estimated from metallurgical examinations and because there is uncertainty about when the additional rubble on top of the hard layer relocated, no further assessment of the impact of the rubble on vessel thermal response was performed.

A model was developed to estimate heat transfer to the vessel from jet impingement and natural convection in the molten pool.[17] The model assumes that one jet impinges at the center of the lower head and a crust forms on the lower head as soon as the melt contacts it. Heat is then transferred through the crust to the vessel at locations where the melt is in contact with the vessel. When the molten jet stops draining and surface agitation is reduced, a crust may form on pool upper and lower surfaces. An energy balance is used in the model to determine the size of the crusts and melt pool. A detailed description of this model may be found in Refs. 2 and 17.

Sensitivity calculations considered the vessel thermal response using various combinations of upper-bound, lower-bound, and best-estimate values for input parameters, such as debris-to-coolant heat transfer, debris decay heat, debris-to-vessel thermal contact, and heat removal from the vessel. Results from several sensitivity studies revealed a consistent vessel thermal response; namely, the thermal response can be divided into three time periods: (a) an initial localized temperature excursion over the time and location of jet impingement (typically lasts for about 1 minute); (b) a transient vessel heatup (typically lasts for about 1 hour); and (c) a quasi-steady vessel temperature distribution (typically lasts for several hours). Best-estimate input values used for a case with nominal input parameters resulted in global peak temperatures of more than 900 °C, which is inconsistent with metallurgical examination data. Only a case with lower-bound input assumptions results in temperature predictions that are, considering the uncertainty range associated with these predictions, consistent with metallurgical examination data; namely, that global vessel temperatures remain below values at which the material undergoes a transition from ferritic to austenitic steel (727 °C).

Results from jet impingement and vessel thermal response calculations indicate that the magnitude and duration of the hot spot temperatures estimated in TMI-2 vessel examinations could not have been caused by an impinging jet because peak temperatures during melt relocation are typically not predicted to be sustained for more than a few minutes (instead of the 30-minute duration indicated by vessel examinations). Hence it is postulated that hot spot temperatures occurred later in the scenario because of a sustained heat load from debris resting on the lower head. The limited area estimated to have experienced hot spot temperatures suggests that this region was subjected to a localized heat source, such as might occur with a nonhomogeneous debris bed or a localized region with better contact between the debris and the vessel.

Weld Failure–Tube Ejection

Before the performance of a tube ejection analysis, it must be established that the nozzle-to-vessel weld failed. Because it is not known if the hot spot temperatures occurred when the RCS was at high pressure, weld failure calculations were performed with the use of a simple model based on force equilibrium (see part b of Fig. 2) in which it was conservatively assumed that peak temperatures and pressures occurred simultaneously. Metallurgical evidence from TMI-2 examinations indicates that the Inconel penetration welds did not melt.[3] Hence peak temperatures inferred from metallurgical examinations of vessel specimens from the hot spot region (less than 1100 °C)[4] were assumed in these calculations. The maximum value of RCS pressure measured after melt relocation, 15 MPa, was assumed for system pressure in these calculations. Shear stress at the weld–tube interface was calculated, converted to effective stress, and used in the MTF calculations.

Results indicate that, even for these conservative assumptions, there was considerable margin in the weld's integrity. Nominal case calculations based on nominal input indicate that the ultimate-strength MTF is 60%. Lower- and upper-limit estimates of the ultimate-strength MTF were 54 and 65%, respectively. If the peak hot spot

temperature and a 15 MPa system pressure were both maintained constant, the time to creep failure is estimated as 7.2 hours with upper and lower estimates of 4.2 and 16.9 hours, respectively. The large ultimate-strength MTF and the long estimated time to creep failure are conservative for several reasons. One reason is that the analysis assumed a constant pressure of 15 MPa, whereas the peak temperatures may have occurred at a lower pressure. Furthermore, calculations assumed that the peak temperature remained constant when, in fact, the peak temperature was estimated to last for only 0.5 hour.[4] In addition, the load-bearing weld area was minimized by ignoring the weld buildup material above the stainless steel cladding and using a minimum weld depth into the vessel. Finally, the load was assumed to be carried solely by the weld, and none of the load was distributed to the tube support located beyond the tube bend outside the vessel. Because penetration weld integrity during the TMI-2 accident was predicted in this very conservative analysis, penetration tube ejection was ruled out as a possible failure mode.

Global Vessel Failure

Two models were used to assess vessel structural response. The first is a simpler, one-dimensional (1-D) model imposing global force equilibrium in spherical geometry, and the second is a more sophisticated, two-dimensional (2-D) model. The 1-D model was applied to provide an initial, rough estimate of failure times. Although this model was quicker and easier to apply, uncertainties associated with 2-D and stress redistribution effects required the more detailed 2-D model.

In the 1-D model, average radial and hoop components of stress are used to define effective stress, as formulated by Huddleston.[18] Creep damage is tracked as a function of stress and temperature at 20 equally spaced layers through the thickness of the vessel. Damage within a particular time interval and at a given location is defined on the basis of the effective stress and temperature through the use of a Larson–Miller Parameter (LMP).[19] The LMP is used to obtain a rupture time, t_r, under the stress and temperature conditions. Incremental damage, d, within a time increment, Δt, is defined as $d = \Delta t/t_r$. As the thermal transient proceeds, the accumulated damage is summed from the incremental damage. When the accumulated damage exceeds unity in a particular layer, that layer of the vessel is removed from the calculated load carrying capacity of the vessel. As discussed previously, MTF is defined as the difference between unity and the ratio of load to load-carrying-capacity. As more layers experience 100% damage, the load-carrying-capacity continues to diminish. Vessel failure is defined as the time when MTF becomes zero.

The 2-D model is an axisymmetric variation of a finite deformation shell theory described in Ref. 20, and the details of the adopted form of the method are described in Ref. 9. The shell theory allows for thermal, plastic, and creep as well as elastic strains but is not as general as an axisymmetric continuum model in that the radial stress is neglected, normal strains are assumed to vary linearly through thickness, and shear strains are assumed to vary parabolically through thickness. The assumed through-thickness behavior permits enforcement of vertical and horizontal force equilibrium and moment equilibrium through integrated force and moment resultants.

Implementation of the stress-based failure criterion in the 2-D model differs slightly from that used in the 1-D model. In the 2-D model, the vessel is divided in the radial direction into ligaments; ligament behavior is allowed to vary continuously in the meridional direction. Stress can vary in both the radial and meridional directions, whereas the simpler 1-D model uses average radial and hoop stresses. Incremental and accumulated damage are evaluated the same way for both models, but when a ligament becomes fully damaged in the 2-D model, it is "clipped," which means the stress state is set to zero and equilibrium necessitates redistribution of stresses to the remaining, intact ligaments. In this stress-based criterion, failure occurs when all the ligaments become fully damaged through thickness at any one location.

Figure 5 compares results from the 1-D model and the 2-D model for the vessel subjected to lower-bound heat fluxes. Parts a and b of Fig. 5 illustrate output from the 1-D model. These parts illustrate the phasing of vessel wall temperature, system pressure, the calculated MTF history, and the timing of vessel layer failure during the accident. As shown in part a of Fig. 5, MTF starts at 80%, reduces to approximately 45% at the 2-hour mark, and quickly drops to 0.0% afterward. Layers of the vessel start to fail after 2.0 hours, and all the layers have failed at 2.3 hours (part b of Fig. 5). Thus the 1-D model predicts failure in slightly less than 2.3 hours.

Part c of Fig. 5 illustrates accumulated damage as calculated from the 2-D model. Damage is defined in the 2-D model as the *average* of the damage evaluated at all integration points along the shell's meridian, so accumulated damage never exceeds unity. This definition is more appropriate for the 2-D model because the number of nodes is variable. As discussed previously, failure is defined in the 2-D model as the time when all the ligaments become fully damaged at any one location

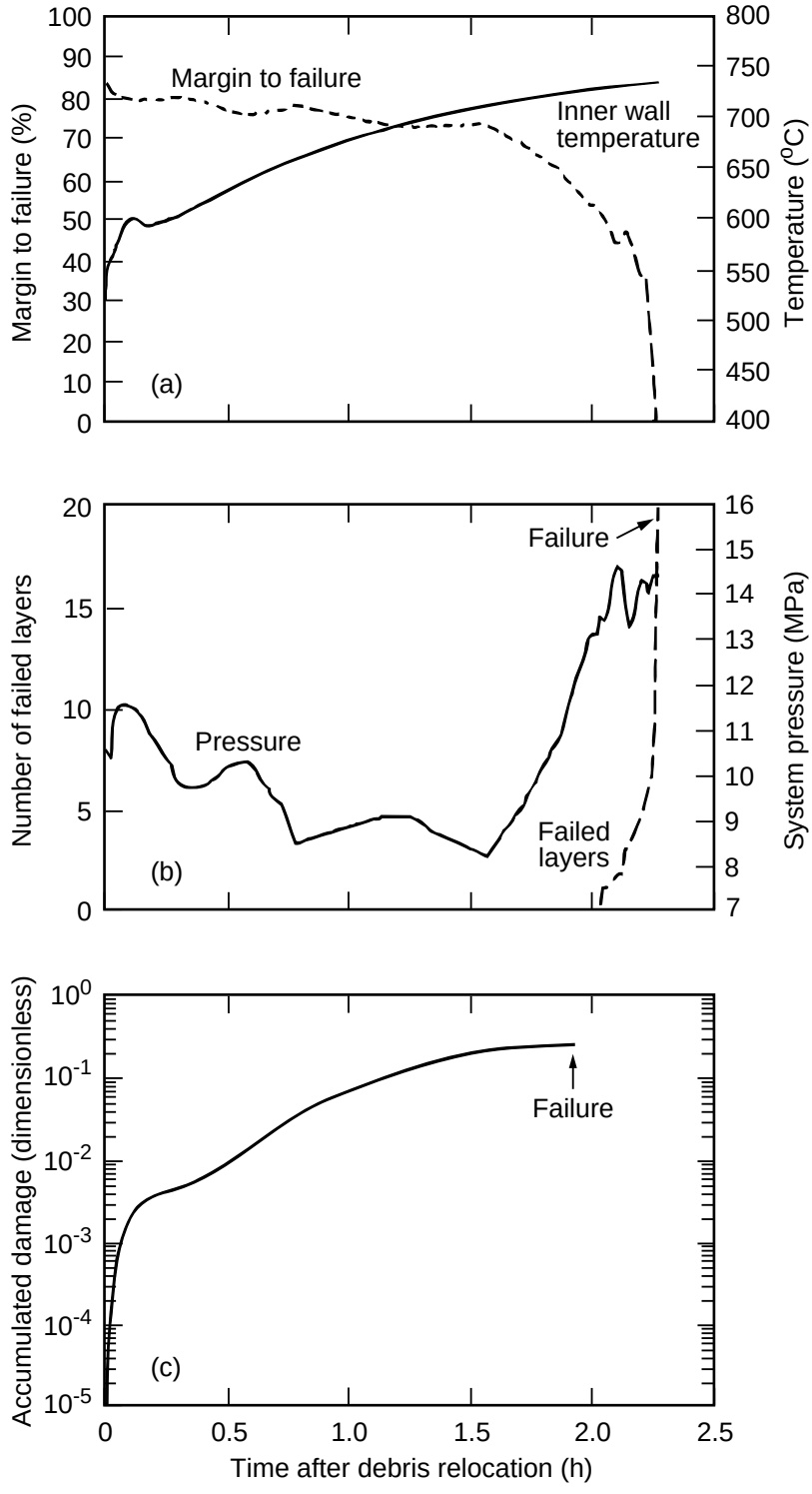

Fig. 5 Comparison of one- and two-dimensional model results for lower-bound case: (a) MTF (1-D model), (b) number of failed layers (1-D model), and (c) accumulated damage (2-D model).

along the shell's meridian. The 2-D model predicts failure at approximately 1.9 hours.

Temperature distributions based on input from companion debris sample examination data (i.e., slow cooling of debris) resulted in calculations from both models predicting vessel failure. Although the inclusion of stress redistribution and 2-D effects in the 2-D model decreased failure predictions by approximately 0.4 hour, both models predict vessel failure at approximately 2 hours. Obviously, this did not occur. Hence it appears that global vessel temperatures must have decreased within 2 hours after core relocation. Hence it is postulated that additional debris cooling, not modeled in these initial calculations based on companion debris sample examination data, occurred within the first 2 hours after melt relocation.

Localized Vessel Failure

The potential for the vessel to experience a localized failure was also evaluated by application of an elevated heat flux over a localized region, which resulted in temperatures and temperature gradients consistent with metallurgical observations of the TMI-2 vessel steel samples.[4] The 2-D structural model used in the global vessel failure analyses was applied to calculate thermal, plastic, and creep strains when the vessel is subjected to a localized heat source.

To understand the relative roles of the hot spot temperature distribution and the global background temperature distribution outside the hot spot, two cases were considered: (a) hot spot temperatures imposed on top of global temperatures estimated for the lower-bound case (see discussion in Jet Impingement/Vessel Thermal Response) and (b) hot spot temperatures imposed on a vessel with cool background temperatures (327 °C inner surface, 277 °C outer surface). These two temperature distributions bounded possible background distributions inferred from vessel steel sample examinations. In these calculations, failure was predicted to occur in 1.5 hours for Case (a), and the vessel was predicted to survive for Case (b).

The effect of a hot spot was evaluated for a shell with a cool background [Case (b)] to confirm that the metallurgically estimated hot spot temperatures alone would not result in a localized vessel failure. Because metallographic examinations of vessel specimens outside the hot spot indicated only that the vessel did not reach the ferritic-to-austenitic transition temperature (approximately 727 °C), global vessel temperatures could have been considerably lower than this transition temperature. (Note that peak values predicted in the lower-bound temperature distribution were approximately equal to the transition temperature.) The initial temperature distribution from the lower-bound case was used to bound possible temperatures in this cooler case; that is, a linear temperature distribution through the thickness with a 327 °C inner surface and a 277 °C outer surface.

The structural response results for Case (b) are in Fig. 6, which shows damage rate vs. time. Note that for the 2-D structural model damage is defined in the 2-D model as the

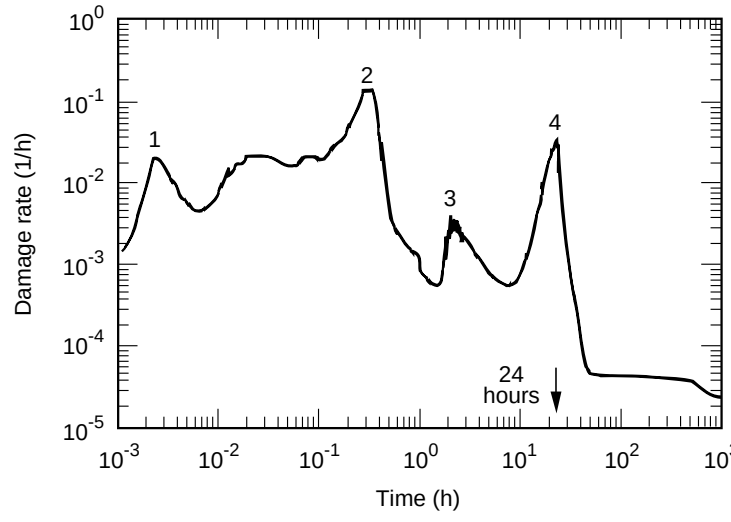

Fig. 6 Damage rate vs. time for localized failure analysis of hot spot temperatures on a cool background.

average of the damage evaluated at all integration points along the shell's meridian. Four important peaks, labeled 1 through 4 in Fig. 6, are in the damage rate.

The first peak (point 1 in Fig. 6), which occurs between 3 and 30 seconds, was associated with the thermal shock (i.e., the nodes on the inner surface experienced a relatively severe damage rate as they reached temperatures in excess of 1027 °C, yielding in compression as they expanded against the cooler shell). This severe damage rate was diminished as the temperature front moved into the interior wall of the vessel.

The second peak (point 2 in Fig. 6) occurs at just over 1000 seconds into the transient and represents the largest rate (0.1 h^{-1}) at any time during the transient. This state occurred when the temperature front had elevated the outer surface temperatures to levels of 527 to 577 °C. The outer surface material was supporting a large tensile stress (~250 MPa) and at this temperature experienced both a high damage rate and creep rate. The damage rate dissipated when the temperature front completely penetrated the shell and thus pushed the outer surface temperature above 727 °C, which reduced the temperature gradient and associated stresses.

At 1.6 hours into the TMI-2 transient, the system was repressurized, and the damage rate experiences a third peak (point 3 in Fig. 6), although of substantially lesser size than the transient heat-up peak. The fluctuations in the repressurization peak mirror the fluctuations in the TMI-2 pressure history associated with relief valve opening and reseating. Although the transient pressure fluctuations continued until 260 minutes after relocation, these calculations assumed a constant pressure for time periods greater than 180 minutes after relocation and thus caused the fluctuations to disappear from the damage rate plot after this time. Repressurization to 14.5 MPa at 2.1 hours also corresponds to the attainment of maximum temperatures in the shell, so the damage rate decreased shortly after repressurization as the shell cooled.

The final damage rate peak (point 4 in Fig. 6) occurs approximately 24 hours after the major melt relocation occurred and is associated with cooldown. During the heat-up and high-temperature periods, material near the inner surface of the vessel at its base experienced compressive stress and underwent negative creep strain under compressive load. As the vessel cooled, this material then contracted and experienced tension. As the material temperature dropped during the cooldown period, tensile stresses on the bottom inner surface exceeded +100 MPa and thus caused rapid damage accumulation and the damage rate peak at 24 hours, which is shown in Fig. 3.

The Structural Mechanics Peer Review Group[7] defined MTF for creep to be the difference between time to failure and the time at which pressure and temperature states are fixed at points of maximum damage rate. Hence the MTF for this case was evaluated by assuming constant temperature and pressure conditions for each of the peaks in Fig. 3 and predicting time to failure, as discussed in the Approach. The initial peak associated with the thermal shock (during melt relocation) was not relevant to the MTF analysis because only the material on the inner surface experienced elevated temperatures during the first 30 seconds of the transient. Hence MTF for this case is the minimum failure time estimated in MTF calculations for peaks 2, 3, and 4 in the damage rate curve. The minimum MTF was obtained by fixing the pressure and temperature conditions corresponding to peak 3. The MTF for this is estimated at 8 hours.

The cases examined in this localized vessel failure analysis indicate that background temperatures play a pivotal role in determining whether the vessel is predicted to survive. The vessel is predicted to fail when hot spot temperatures are superimposed on a global temperature distribution obtained with heat fluxes corresponding to lower-bound input assumptions; however, the vessel can survive local hot spots in the temperature range and of the duration inferred from TMI-2 metallurgical examinations, but the balance of the shell must remain cool.

Sensitivity to Debris Cooling and Failure Criterion

As noted previously, thermal analyses were performed on the basis of debris properties (decay heat levels, "slow cooling" evidence) from the companion debris sample examinations; however, thermal and structural calculational results combined with metallurgical examination results suggest the hypothesis that some form of cooling occurred that was not evident in the TMI-2 companion debris samples. In addition, analysis results suggest that the stress-based failure criterion that is used to predict failure may be too conservative. Analyses performed to investigate the effects of debris cooling and failure criterion on calculational results are discussed in the following text.

Changes in Debris Internal Energy After Relocation

Initial scoping calculation results suggest that some form of debris cooling occurred within the vessel after a major relocation occurred (approximately 224 minutes)

and before the vessel was repressurized (approximately 320 minutes). Through the application of some simplifying assumptions related to heat transfer within the vessel, equations for volume, mass, and energy conservation were used to obtain an order-of-magnitude estimate of the change in debris internal energy after debris relocation. Sources of coolant entering the vessel during the time period of interest include normal RCS makeup and high-pressure injection from the emergency core cooling system. Sources of coolant exiting the vessel during this time period include normal RCS letdown and coolant flowing out the open power-operated relief valve (PORV). These coolant flow rates and associated uncertainties were quantified with results from previous analyses of plant data.[21–24] The amount of decay heat input to the system was quantified with information in Ref. 25 to account for the reduction caused by volatile fission-product release.

Calculation results indicate that the debris internal energy decreased between relocation and vessel repressurization. Calculations considered upper and lower bounds for all the input parameters, such as coolant flow rates entering and exiting the vessel and debris decay heat levels. Hence results from these scoping calculations should be viewed as order-of-magnitude estimates; however, results indicate that a negative change in debris internal energy occurred for the time period of interest in all the cases considered and support the hypothesis that debris cooling occurred that was not evident in the TMI-2 companion debris samples. Although considerable uncertainty is associated with these results, scoping calculations suggest that the estimated decrease in debris internal energy is sufficient for all the debris that relocated to the lower head to solidify and experience a decrease in temperature ranging from 420 to 2250 °C.

Slow and Rapid Cooling Analysis

Although there are insufficient data from the companion debris samples to determine the exact mechanisms that caused the rapid cooling of the debris within the first 2 hours after relocation, two possible forms of cooling were investigated. The first form of cooling considered was a slow cooling mode in which channels or cracks in the debris allowed for infusion of water that cooled the debris near the channels but left interior portions hot. This slow cooling was investigated by analyzing cases with a hot spot temperature distribution superimposed on 25, 33, and 50% of the background heat fluxes obtained using nominal case input values. Results, summarized in part a of Fig. 7, indicate that the vessel would fail at 2.6 hours for a hot spot on a background equal to 50% of nominal case heat flux, but the vessel would survive on a background of 25% of nominal case heat flux. For the 33% of nominal case, results in part a of Fig. 7 indicate that the damage rate begins to rise during the repressurization period, which implies that failure is imminent. Depressurization 4 hours into the transient enables the vessel to survive a couple of hours longer, but ultimately the vessel is predicted to fail at 6.5 hours after melt relocation. These results indicate that, under slow cooling conditions and with a stress-based failure criterion, the vessel can survive a hot spot in the presence of background heat fluxes between 25 and 33% of nominal values.

The second form of cooling considered was a rapid cooling mode in which gaps or channels between the lower debris crust and the vessel allowed relatively high flow rates of coolant between the debris and the vessel. (These high flow rates rapidly cooled the vessel and outer portions of the debris but left interior portions of the debris relatively hot.) Analyses were performed to investigate the cooling needed to obtain vessel cooling rates consistent with the values observed in metallurgical examinations of specimens in the hot spot region, namely, that vessel specimens from the hot spot region underwent cooling rates between 10 and 100 °C/min in the ferritic-to-austenitic transition temperature region (727 to 827 °C) at approximately 30 minutes after the hot spot reached 1047 °C. Rapid cooling calculations were performed for cases of hot spot temperatures on 33 and 50% of nominal background heat fluxes. The heat sinks required to obtain these cooling rates were 25 and 125 kW/m^2, respectively. Under rapid cooling conditions, it is concluded that the structure must be close to failure before initiation of cooling for the vessel to subsequently fail. For these conditions, additional damage or strain accumulated during the cooldown period is minimal. The difference between cooling rates is exhibited in the timing and magnitude of damage peaks associated with cooldown. The faster cooling rate produces higher tensile stresses earlier in the transient, which results in an earlier and larger damage rate peak. Unlike the case illustrated in Fig. 6, however, the structure moves through this peak quickly, with little additional accumulated damage, and the damage rate then falls rapidly to a benign level. Simulations were also run for a hot spot on 75% of the nominal heat flux, but these simulations predict vessel failure in a little over 2 hours. Hence the vessel can survive a hot spot in the presence of background heat fluxes between

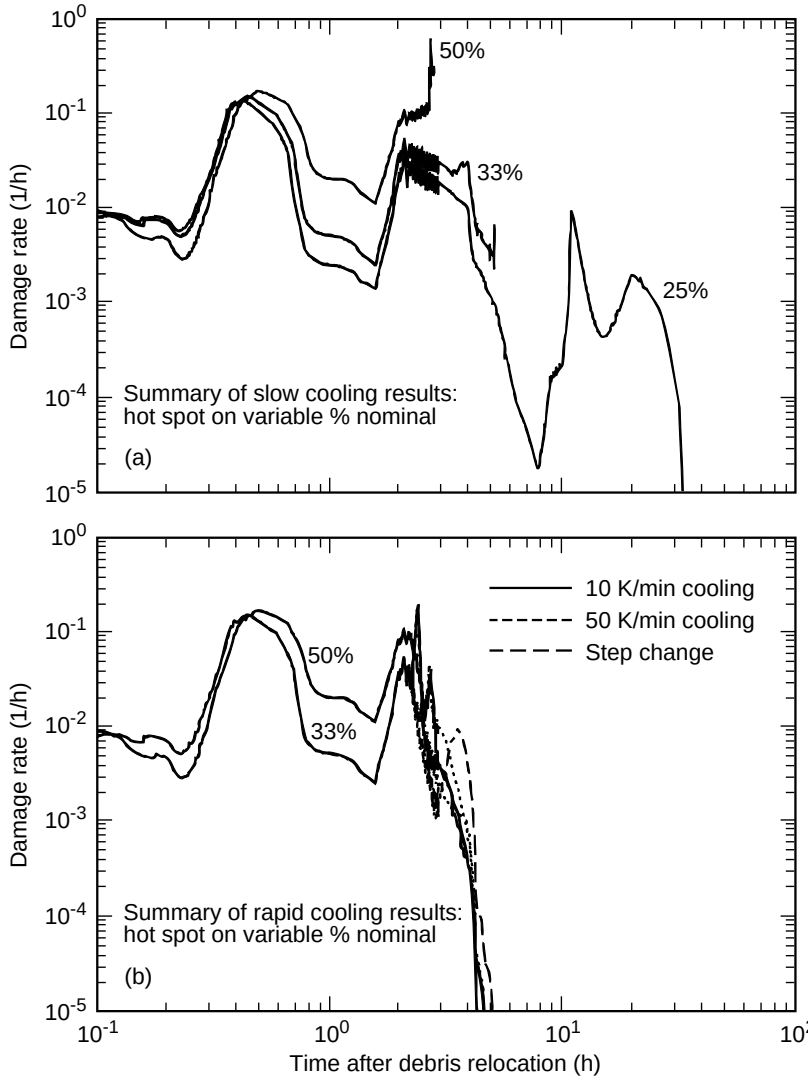

Fig. 7 Summary of slow and rapid cooling results obtained with a stress-based failure criterion: (a) slow cooling results and (b) rapid cooling results.

50 and 75% of the nominal case heat fluxes during the 30-minute time interval that hot spot temperatures are sustained and before the initiation of rapid cooling.

In summary, analyses indicate that both slow and rapid cooling occurred in some debris locations during the first 2 hours after melt relocation. If only a slow cooling mechanism were present, the vessel temperatures would not experience the rapid cooling rates observed in the metallurgical examinations. Furthermore, the vessel will not survive hot spot temperatures on the nominal case heat fluxes long enough to permit material to exist at elevated (>1050 °C) temperatures for the 30-minute time period estimated in metallurgical examinations. Thus analyses indicate that both slow and rapid cooling mechanisms must be considered to obtain results consistent with TMI-2 VIP examinations.

Configurations to Obtain Required Cooling Rates

Although there are insufficient data to quantitatively determine the exact cooling mechanisms required to obtain a vessel response consistent with metallurgical data, scoping calculations were performed to investigate the potential for channels and gaps within the debris to

cause this cooling (the presence of this cooling would allow consistency of the companion debris sample data, the vessel steel sample data, and the thermal and structural response analyses). Estimating the number and size of debris channels and the size of debris-to-vessel gaps requires many assumptions related to debris properties and heat transfer parameters. This large uncertainty in input parameters was treated by estimating upper and lower bounds for each parameter and obtaining results by propagating upper- and lower-bound estimates. Lower-bound geometric parameters for channels within the debris and between the debris and the vessel were selected to minimize heat transfer capabilities. As discussed previously, results indicate that both rapid and slow cooling mechanisms were needed to be consistent with metallurgical examination data. Therefore it is assumed that the simultaneous presence of cracks and gaps within the debris provides multiple pathways for steam release (e.g., water may travel down along the gap and boil up through cracks). To maximize the number of cooling cracks and the gap size required to cool the debris, the heat transfer from the debris to the coolant was minimized by assuming that the coolant traveling through these cracks and gaps remained in a liquid state and neglecting any enhanced heat removal associated with subcooled or saturated boiling of the coolant.

Results indicate that a relatively insignificant volume of channels within the TMI-2 debris bed (<1% of the debris volume) could have removed a sufficient amount of heat to preclude vessel failure. Calculations also indicate that coolant traveling through a relatively small gap (a value of 1 mm was assumed) between the debris and the vessel could cause the vessel cooling rates estimated by metallurgical examination data. Although companion debris sample examinations did not substantiate the hypothesis that portions of the debris cooled within the first 2 hours, the mass of the companion debris samples was small compared with the mass that relocated (<7 kg of the 19 000 kg that relocated were examined).

Sensitivity of Results to Failure Criterion

Vessel deformation and damage distributions obtained in the initial scoping calculations indicate that failure strains are quite modest (<10%). For these reasons, the Structural Mechanics Peer Review Group suggested that another set of structural simulations be performed with a failure criterion based upon mechanical instability.[8] Calculations were performed to investigate the influence of failure criterion on the amount of slow cooling needed to preclude vessel failure and the amount of rapid cooling needed to obtain cooling rates consistent with the cooling indicated by metallurgical examinations. The characteristic deformations used to define instability are the maximum hoop strain, u/r_0, located underneath the hot spot; the maximum vertical deflection, w, also located under the hot spot; and the maximum rotation of the shell meridian from its undeformed state, β, located somewhere in the cusped region of the undeformed shell.

In the slow cooling calculations, simulations were performed involving the hot spot on background heat flux distributions corresponding to 100, 75, 62.5, and 50% of the nominal case. Results for the 62.5 and 50% nominal cases are shown in part a of Fig. 8. For the 50% nominal case, the bulk of the vessel remains sufficiently stiff to restrain the hot spot region; consequently, tensile stresses in the hot spot region 4 hours after relocation are quite modest. When the system depressurizes at 4 hours, the vessel unloads elastically, and most of the vessel under the hot spot subsequently experiences compression. Under these conditions, the vessel creeps down in the hot spot region and u/r_0 decreases. Maximum values of w and β remain nearly constant.

Deflections for the case with 62.5% nominal are substantially greater than those for the case with 50%. When the vessel is less restrained, more tension exists, and no discernible decrease in hoop strain occurs when the pressure decreases. Once depressurization stops at 5.25 hours, the deformations again begin to increase. The increasing deflections near 6 hours for the 62.5% case suggest, however, that it is unlikely the vessel would survive upon complete repressurization to 16 MPa at 11 hours. It is concluded that, under slow cooling conditions and a deformation-based criterion, the vessel can survive a hot spot on a background heat flux between 50 and 62.5% of the nominal level.

In the rapid cooling calculations, simulations were performed for hot spots on background heat fluxes equal to 62.5, 75, and 80% of the nominal level. Results in part b of Fig. 8 indicate that the vessel easily survives rapid cooling from 62.5% of nominal, and all deformations asymptotically settle to benign values. When rapid cooling is initiated from hot spots on 75% of nominal, however, the vessel has already experienced substantial deformation before initiating cooling. The inspection of curves in part b of Fig. 8 indicates that during the cooling period the rotation β actually decreases but then begins to climb again once cooling is completed. The depressurization period between 4 and 11 hours greatly slows the rate of vessel deformation, but repressurization to 15 MPa at 11 hours causes the deformation to increase dramatically.

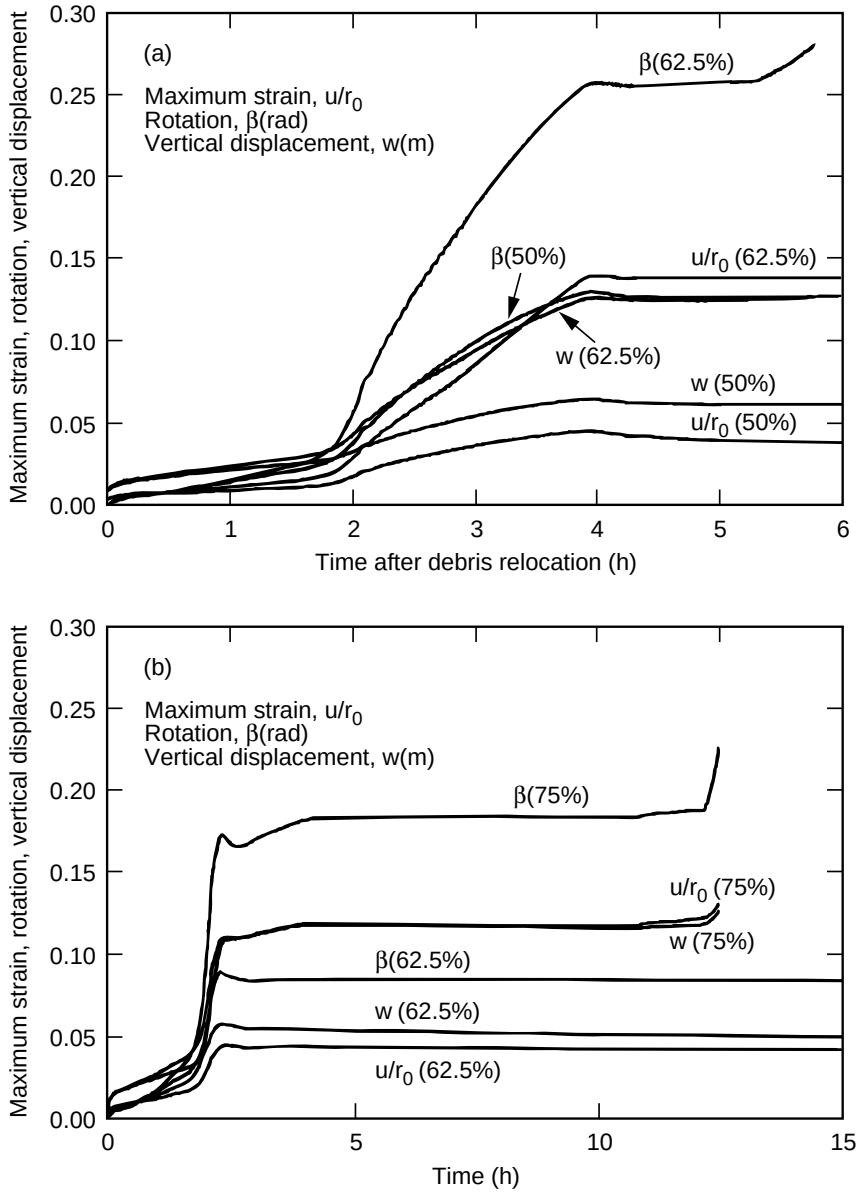

Fig. 8 Results obtained with a deformation-based criterion: (a) slow cooling results and (b) rapid cooling results.

It appears that under rapid cooling hot spots on 75 and 80% of nominal background heat fluxes cause failure in approximately 13 and 11 hours, respectively. Therefore it is concluded that, under rapid cooling conditions and the deformation-based criterion, the vessel can survive a hot spot on a background heat flux between 62.5 and 75% of nominal.

SUMMARY

Data available from the OECD-sponsored TMI-2 VIP, plant instrumentation during the accident, and previous TMI-2 research programs were used to estimate the MTF that existed in the vessel during the accident. These data also provided a unique opportunity to evaluate the predictive capability of severe accident analysis models for

which limited validation data exists. The MTF analysis effort of the VIP included calculations to consider four vessel lower-head failure mechanisms: penetration tube rupture, penetration tube ejection, global vessel rupture, and localized vessel rupture.

Analyses results indicate that tube rupture and tube ejection could be eliminated as potential failure mechanisms during the TMI-2 accident. Global vessel failure analyses suggest that significant debris cooling, not considered in severe accident analysis models, must have occurred within approximately 2 hours after debris relocation to the lower head. Analyses also indicate that additional data are needed to select an appropriate vessel failure criterion because the magnitude of cooling required to obtain vessel temperatures consistent with values inferred from vessel steel examinations was sensitive to the failure criterion used in structural response calculations. Although examinations of companion debris samples did not provide supporting evidence of this additional debris cooling, metallurgical examinations did provide evidence that this cooling occurred in the hot spot location. Localized vessel failure analyses indicate that it is possible for the vessel to withstand the hot spot temperatures for time periods inferred from VIP metallurgical examinations provided that the balance of the vessel is relatively cool. Although there are insufficient data to determine the exact mechanisms that caused the debris to cool, scoping calculation results indicate that a minimal volume of cooling channels within the debris and a minimal size gap between the debris and the vessel could supply the cooling needed to obtain vessel temperatures and cooling rates determined in metallurgical examinations.

REFERENCES

1. ASME, Use of SA-533 Grade B, Class 1 Plate and SA-508 Class 3 Forgings and Their Weldments for Limited Elevated Temperature Service, Sect. III, Division 1, Cases of ASME Boiler and Pressure Vessel Code, Case N-499, Approved December 16, 1991.
2. L. A. Stickler et al., *Calculations to Estimate the Margin to Failure in the TMI-2 Vessel*, Report NUREG/CR-6196 (EGG-2733) [TMI V(93) EG01], October 1993.
3. D. R. Diercks and L. A. Neimark, *Results of Mechanical Tests and Supplementary Microstructural Examinations of the TMI-2 Lower Head Samples*, Report NUREG/CR-6187 (ANL-94/8) [TMI V(93)AL02], June 1993.,
4. G. E. Korth, *Metallographic and Hardness Examinations of TMI-2 Lower Pressure Vessel Head Samples*, Report NUREG/CR-6194 (EGG-2731) [TMI V(92)EG01], January 1992..
5. D. W. Akers, S. M. Jensen, and B. K. Schuetz, *Companion Sample Examinations*, Report NUREG/CR-6195 (EGG-2732) [TMI V(92)EG10], July 1992.
6. L. A. Neimark, T. L. Shearer, A. Purohit, and A. G. Hins, *TMI-2 Instrument Nozzle Examinations at Argonne National Laboratory*, Report NUREG/CR-6185 (ANL-94/5) [OECD-NEA-TMI-2 V(93)AL01], February 1993.
7. J. Strosnider, *Summary Record of the TMI VIP Structural Mechanics Peer Review Group Meeting, Idaho Falls, Idaho, May 11, 1992*, TMI V(92) EG09, OECD-NEA-TMI-2 Vessel Investigation Project, July 20, 1992.
8. Y. R. Rashid, Summary of Comments on the Margin-to-Failure Report, Presentation at the 11th Programme Review Meeting of the OECD-NEA-TMI-2 Vessel Investigation Project, TMI V(93)MAN17.
9. J. L. Rempe, S. A. Chavez, and G. L. Thinnes, *Light Water Reactor Lower Head Failure Analysis*, Report NUREG/CR-5642 (EGG-2618), October 1993.
10. R. W. Ostensen and J. F. Jackson, Extended Fuel Motion Study, in *Reactor Development Program Progress Report*, Report ANL-RDP-18, pp. 7.4-7.7 July 1973.
11. R. W. Ostensen, R. E. Henry, J. F. Jackson, G. T. Goldfuss, W. H. Gunther, and N. E. Parker, Fuel Flow and Freezing in the Upper Subassembly Structure Following an LMFBR Disassembly, *Trans. Am. Nucl. Soc.*, 18: 214-215 (1974).
12. M. Epstein, Transient Freezing of Flowing Ceramic Fuel in a Steel Channel, *Nucl. Sci. Eng.*, 61(3): 310-323 (1976).
13. M. Epstein, Heat Conduction in the UO_2-Cladding Composite Body with Simultaneous Solidification and Melting, *Nucl. Sci. Eng.*, 51(1): 84-87 (May 1973).
14. Personal communication with Norman Cole, MPA Associates, Inc., Washington, D.C., October 1992.
15. H. Warren, *Interpretation of TMI-2 Instrument Data*, Report EPRI-NSAC-028, May 1982.
16. C. C. Chu, M. L. Corradini, J. Murphy, and J. Tang, *A Code Manual for TEXAS-II: One-Dimensional Transient Fluid Model for Fuel/Coolant Interaction Analysis*, Report UWRSR-39, July 1992.
17. J. A. Kos, Model of Fuel-Melt Quenching in the Lower Plenum of the RPV, M.S. Thesis, University of Wisconsin, Madison, Wisconsin, August 1992.
18. R. L. Huddleston, An Improved Multiaxial Creep-Rupture Strength Criterion, *Am. Soc. Mech. Eng., Pressure Vessel Technology*, 107: 421-429 (1985).
19. F. R. Larson and J. Miller, A Time–Temperature Relationship for Rupture and Creep Stress, *Trans. ASME*, 765-775 (July 1952).
20. S. Lin, T. Lin, and B. Mazelsky, Large Deflection of Axisymmetric Shell with Creep Strain, *J. Eng. Mech.*, 100: 79-94 (1974).
21. J. L. Anderson, *Recommended HPI Rates for the TMI-2 Analysis Exercise (0–300 Minutes)*, Report EGG-TMI-7833, EG&G Idaho, Inc., September 1987.
22. P. Kuan and E. L. Tolman, *Electromatic Relief Valve Flow and Primary System Hydrogen Storage During the TMI-2 Accident*, Report EGG-TMI-7703, EG&G Idaho, Inc., May 1987.
23. R. D. McCormick, J. L. Anderson, and D. W. Golden, *TMI-2 Data Summary Report*, Report EGG-TMI-7843, EG&G Idaho, Inc., September 1987.
24. Y. Nomura, *PORV Discharge Flow During the TMI-2 Accident*, Report EGG-TMI-7825, EG&G Idaho, Inc., July 1987.
25. B. G. Schnitzler, *Fission Product Decay Heat Modeling for Disrupted Fuel Regions (FDECAY)*, Report EGG-PHYS-5698, EG&G Idaho, Inc., December 1981.